Annals of Forest Science (2012) 69:399–408
DOI 10.1007/s13595-011-0164-1

ORIGINAL PAPER

The effect of the G-layer on the viscoelastic properties of tropical hardwoods

J. Paul McLean · Olivier Arnould · Jacques Beauchêne · Bruno Clair

Received: 30 May 2011 / Accepted: 15 November 2011 / Published online: 13 January 2012

Abstract
• ***Context and aim*** This study aimed to examine the effect of the tension wood G-layer on the viscoelastic properties of wood.
• ***Methods*** Tension wood and opposite wood samples were obtained from six French Guianese tropical rainforest species (*Sextonia rubra*, *Ocotea guyanensis*, *Inga alba*, *Tachigali melinoni*, *Iyranthera sagotiana* and *Virola michelii*); the tension wood of the former three of these species had a G-layer, whilst the tension wood from the latter three had no G-layer. Tensile dynamic mechanical analysis (DMA) was performed on green never dried wood samples in the longitudinal direction with samples submerged in a water bath at a temperature (30°C) and frequency (1 Hz) representative of the conditions experienced by wood within a living tree. Then, DMA was repeated with samples conditioned to an air-dried state. Finally, samples were oven-dried to measure longitudinal shrinkage.
• ***Results*** Tension wood did not always have a higher longitudinal storage (elastic) modulus than opposite wood from the same tree regardless of the presence or absence of a G-layer. For the species containing a G-layer, tension wood had a higher damping coefficient and experienced a greater longitudinal shrinkage upon drying than opposite wood from the same species. No difference was found in damping coefficients between tension wood and opposite wood for the species that had no G-layer.
• ***Conclusion*** It is proposed that the different molecular composition of the G-layer matrix has an influence on the viscoelasticity of wood, even if a biomechanical gain is not yet clear. This study shows that rheological properties and longitudinal shrinkage can be used to detect the presence of a G-layer in tension wood.

Keywords DMA · G-layer · Reaction wood · Tropical wood · Viscoelasticity

Handling Editor: Barry Alan Gardiner, PhD

Contribution of co-authors J. Paul McLean: Preparation of samples, mechanical and physical measurements, analysis of data and writing of the manuscript.
Olivier Arnould: Conception of the experiment, particularly the mechanical measurements, assistance with DMA apparatus and participation in manuscript.
Jacques Beauchêne: Assistance in locating, collecting and preparing sample material; participation in presentation; and discussion of results.
Bruno Clair: Conception of the experiment, field measurement of maturation strain, collection of material, participation in manuscript and general supervision.

J. P. McLean · O. Arnould · B. Clair
Laboratoire de Mécanique et Génie Civil (LMGC),
Université Montpellier 2, CNRS,
Montpellier, France

J. P. McLean (✉)
Forest Products Research Institute, Edinburgh Napier University,
Merchiston Campus,
Edinburgh EH10 5DT, UK
e-mail: p.mclean@napier.ac.uk

J. Beauchêne
UMR Ecologie des Forêts de Guyane (ECOFOG), CIRAD,
Kourou, French Guiana

1 Introduction

Reaction wood is formed in response to mechanical stress that has caused vertical misalignment of the tree stem. Such stress arises from: (1) uneven self-loading, for example due to weight overhang (Yoshida et al. 2000) resulting from

non-symmetrical crown growth or growth on sloping ground, and (2) external factors such as wind loading (Tanaka et al. 1981). Tension wood (TW), the name given to reaction wood produced by angiosperm trees, is found on the upper side of the leaning stem. As the name implies, TW creates a tensile force somewhat higher than that of the geometrically opposing (opposite) wood (OW) within the same tree (Fisher and Stevenson 1981; Wardrop 1964), with the result that the stem will be bent towards the side with the higher force (i.e. towards the TW). In order to perform its function, the anatomical (Jourez et al. 2001; Ruelle et al. 2006) and mechanical properties (Clair et al. 2003; Coutand et al. 2004; Fang et al. 2008; Ruelle et al. 2007) of TW can be very different from those of OW. A remarkable anatomical feature of TW in some species is the gelatinous G-layer (Clair et al. 2006; Onaka 1949), which is deposited after the S2 layer during cell differentiation (Clair et al. 2011). However, this G-layer is not present in the TW of all species (Chang et al. 2009; Clair et al. 2006), and thus we can make a simple anatomical distinction between the G-layer and non-G-layer TW.

There is still some debate as to the actual molecular composition of the G-layer. To date, the literature shows that the G-layer is composed of mostly (~90%) highly crystalline cellulose (Daniel et al. 2006; Nishikubo et al. 2007; Norberg and Meier 1966). These cellulose aggregates are embedded in a matrix containing xlyoglucans (Baba et al. 2009; Nishikubo et al. 2007) and aribinogalactans, in which lignin is absent (Donaldson 2001) or occurs only in trace amounts (Joseleau et al. 2004). In contrast, the S2-layer of normal wood consists of ~59% cellulose crystal aggregates in a matrix consisting of ~14% non-cellulosic polysaccharides and ~27% lignin (Fengel and Wegener 1984).

In G-layer tension wood, the greater the quantity of G-layer, the higher the tensile maturation stress (Fang et al. 2008). However, there is apparently no difference in maturation stresses between G-layer and non-G-layer-producing species (Clair et al. 2006). Therefore, the benefit of a G-layer to the living tree is currently unknown.

Mechanical research into TW has until now mainly focused on the axial elastic modulus. However, wood, like other polymeric composite materials, displays viscoelastic behaviour (Navi and Stanzl-Tschegg 2009). By definition, the mechanical response of a viscoelastic material contains both elastic (instantaneous) and viscous (time-dependant) elements. After loading and upon unloading, a purely elastic material will immediately return to its initial state, giving back all the mechanically applied energy, whilst a purely viscous material will show a delay in response, never return to its initial state and dissipate all the applied energy. Therefore, a viscoelastic material will return part of the applied energy, with a delay in mechanical response, and dissipate the rest. Wood elasticity is mainly obtained from the stiffness and orientation of the crystalline cellulose microfibrils (i.e. microfibril angle or MFA) within the secondary wall (Cave 1968; Salmen and Burgert 2009), whilst the origin of wood viscosity is the non-cellulosic polysaccharide matrix (Navi and Stanzl-Tschegg 2009; Salmen and Burgert 2009). Wood viscoelasticity is anisotropic and highly dependent upon temperature and moisture content (Navi and Stanzl-Tschegg 2009).

In this study, the aim was to observe the effect of the G-layer on the longitudinal viscoelastic properties of TW compared with OW in tropical rainforest species. We hypothesised that the different composition of the G-layer would result in a different viscoelastic response. In order to do so, we performed dynamic mechanical analysis (DMA) on TW and OW of tree species, which either exhibited or did not exhibit a G layer in their TW. We further theorised that any difference in viscoelastic properties could have a biomechanical role within the living tree; thus, initial DMA tests were performed on green wood under conditions resembling those of the living tree.

2 Material and methods

2.1 Material

Sample trees were collected in the vicinity of the Paracou experimental field station (5°18′ N, 52°55′ W), a lowland tropical forest near Sinnamary, French Guiana. Six common species were chosen (Table 1), representing three groups of taxonomically similar species; two trees were sampled per species. Individuals with a crooked or sweeping stem form were chosen to maximise the possibility of TW occurrence. On the standing trees, the asymmetrical trunk stresses associated with reaction wood formation (Trenard and Gueneau 1975) were verified by performing maturation strain measurements at eight points around the circumference at breast height (Fang et al. 2008) using the strain gauge method (Jullien and Gril 2008; Yoshida and Okuyama 2002). Trees were then felled and eight radial sections, matching the locations of the maturation strain measurements, were cut from each. The section corresponding to the highest maturation strain measurement was used to provide TW; the opposite section, in relation to standing tree geometry, displaying the lowest maturation strain measurement was used for OW. Three samples of dimensions 150×2×12 mm^3 ($L \times R \times T$) were cut from the outer (bark side) part of the TW and OW sections of each tree, resulting in six samples per wood type per species. To maintain the green condition, sample material was not allowed to dry out throughout the preparation process. Following preparation, samples were stored in water, in sealed containers, at 4°C. Anatomical measurements, to confirm the presence of TW and identify fibre pattern (presence or absence of a G-layer),

Table 1 Materials used in the study

Family	Species	Tree	Tree diameter at breast height (cm)	GS TW (μm/m)	GS OW (μm/m)	Fibre pattern
Lauraceae	*Sextonia rubra*	A	25	−2,362	−400	G-Thick
		B	21	−1,657	−59	
	Ocotea guyanensis	A	19	−1,870	−585	G-Thin
		B	18	−1,798	−266	
Myristicaceae	*Iyranthera sagotiana*	A	26	−1,485	−305	No G
		B	22	−922	−165	
	Virola michelii	A	36	−1,699	45	No G
		B	37	−232	−7	
Fabaceae	*Inga alba*	A	29	−2,408	−401	G-Thin
		B	17	−2,192	−10	
	Tachigali melinoni	A	18	−1,488	−519	Few or no G
		B	12	−2,112	−653	

There are six species with two trees per species; thus, the values presented refer to individual measurements. Negative GS implies tension and positive GS implies compression. GS measurements were made at eight points around the circumference of the tree; the maximum was chosen to be TW and the geometrically opposite, which displayed the minimum GS as OW

GS maturation stress, TW tension wood, OW opposite wood

were carried out on an adjacent sample material from one of the two sample trees per species (Chang et al. 2009). Maturation strain measurements and fibre characteristics are shown in Table 1.

2.2 Overview of dynamic mechanical analysis

Material viscoelastic properties are commonly measured by DMA (Menard 2008). This technique provides the storage modulus (E') and the loss angle called 'tangent delta' (tan δ). In the case of a material with low viscosity, like wood, E' is close to the elastic modulus of the material, which is directly proportional to the stiffness of the sample. Experimentally, E' is calculated from the ratio of the peak-to-peak range of stress ($\Delta\sigma$) to the peak-to-peak range of strain ($\Delta\varepsilon$) multiplied by the cosine of the phase angle δ, i.e. the phase lag, between the oscillating applied stress and the resulting strain (Fig. 1). Tan δ is representative of the ratio between the dissipated energy and the elastically stored energy during one loading cycle. A purely elastic material will have no phase lag (hence, zero tan δ), whereas a material with a viscous component will have a phase lag relative to the degree of viscosity (up to 90° for a purely viscous material). In the case of a material that is predominantly elastic, like wood, tan δ is considered to be the damping coefficient. In a comparison of materials, a higher relative tan δ indicates a material with a higher relative damping, i.e. a relatively more viscous material.

2.3 Dynamic mechanical analysis of green wood

DMA tests were performed using a BOSE-Electroforce 3230 Dynamic Mechanical Analyser equipped with tensile fatigue grips, a submersible 450 N load cell and a high-resolution displacement sensor (1 mm range). Samples were tensile tested in the longitudinal direction under water by means of a custom-made water bath whose temperature was regulated to 30°C (using a Huber Ministat cc3), a temperature close to the natural environment of the trees in the tropical rainforest. Prior to the mechanical testing, samples were placed in water for more than 2 h at room temperature; then transferred to a water bath at 30°C for a further 2 h. After thermal conditioning, sample dimensions were measured. The sample was then loaded into the grips, which were placed 119 to 129 mm apart; this distance depended on the batch of samples tested as a joint sealing the grip support to water required periodic inspection to prevent leaks. All samples from one species were measured

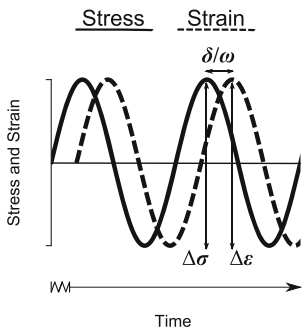

Fig. 1 An example of a sinusoidal loading in dynamic mechanical analysis or DMA. Note that the x-axis (time) does not start at zero and that several cycles have already passed. For a linear viscoelastic material (shown), the imposed sinusoidal stress results in a sinusoidal strain with a time delay of δ/ω, where δ is the phase lag or phase angle between σ and ε, and ω is the angular frequency or periodicity of both sine wave

within one batch. A quasi-static loading, within the elastic limit, was imposed to ensure that there would be no slippage of the sample in the grips during subsequent loading used for the determination of viscoelastic properties. A quasi-static ramp test was again performed on each sample prior to DMA analysis to determine the tensile Young's (or longitudinal elastic) modulus, which was in turn used to calculate the quantity of stress to produce a given strain. The DMA applied a sinusoidal force leading to 0.02% mean strain with oscillating peak-to-peak amplitude of 0.03%, resulting in a range of strain from 0.005% to 0.035%, which was large enough to remain in tension but small enough to remain within the linear viscoelastic domain (Sun et al. 2007). Sinusoidal force was imposed at a frequency of 1 Hz to represent the oscillation of the correct order for a standing tree (Bruchert et al. 2003; Moore and Maguire 2008) whilst remaining in a frequency range where the utilised DMA apparatus and configuration was determined to have a more accurate response (unpublished data). Tan δ was calculated by Fourier transformation analysis within the integral BOSE WinTest™ DMA Analysis software. Values of E' and tan δ were post-corrected for the stiffness of the testing apparatus.

2.4 DMA of air-dried wood and longitudinal shrinkage

Following the DMA tests in the green condition, samples were air-dried, under gentle displacement restraints to prevent distortion, for a period of about 2 weeks until constant mass was achieved. DMA was repeated as above, but without the water bath. Sample grips were always 122 mm apart. Following the DMA tests in the air-dried condition, samples were oven-dried in order to obtain dry mass and length used to calculate basic density (ρ = oven dry mass/green volume), check the moisture content of samples in the air-dried condition and to calculate longitudinal shrinkage between the green and oven-dried conditions.

2.5 Statistical analysis

Analysis of variance (ANOVA) was used to determine whether there was a significant effect of wood type on the specific storage modulus ($E'\rho^{-1}$, i.e. E' normalised for basic density), tan δ, longitudinal shrinkage or basic density (ρ). Data were primarily grouped by species then subdivided into TW or OW (n=6). An F-test was used to determine the significance (α=0.05) of wood type on each variable, and, when appropriate, a post hoc Tukey HSD test was used to examine the within-species differences in means between wood types. This analysis was also carried out on data grouped by species, tree and wood type (n=3). Due to the statistically prohibitive low quantity of individuals sampled per species, interspecies differences were not pursued. Analysis was carried out using the open source R software (R Development Core Team 2011).

3 Results

The $E'\rho^{-1}$ in the green condition is plotted by species and wood type (Fig. 2A). ANOVA showed that wood type was significant (F=121.21, p<0.001). The post hoc Tukey HSD test showed that the $E'\rho^{-1}$ of TW was significantly higher (p<0.001) than that of the OW for *Ocotea guyanensis*, *Inga alba*, *Tachigali meloni* and *Virola michelii* by 4.14, 5.48, 3.54 and 3.98×10^{-6} m^2 s^{-2}, respectively. A similar pattern is observed when analysing the data from individual trees (Table 2), though differences were not always significant.

The $E'\rho^{-1}$ in the dry condition is plotted by species and wood type (Fig. 2B). ANOVA showed that wood type was significant. The post hoc Tukey HSD test showed that the $E'\rho^{-1}$ of TW was significantly higher (p<0.001) than that of the OW for *I. alba*, *T. meloni* and *V. michelli* by 11.61, 6.48 and 5.01×10^{-6} m^2 s^{-2}, respectively. Differences in air-dried $E'\rho^{-1}$ were almost identical to those in the green condition; the exception was that the difference between TW and OW from *Ocotea guyanensis* was no longer significant (p=0.3). Additionally, whilst the $E'\rho^{-1}$ of most species increased upon drying, that of *O. guyanensis* remained of a similar order for OW whilst decreasing slightly for TW, though this was only true for one tree (Table 2). A paired two-sample t test between green and air-dried $E'\rho^{-1}$ showed that this difference was not significant (p=0.2), and therefore drying is considered to have had no effect on the $E'\rho^{-1}$ of *O. guyanensis*.

The mean measured tan δ at 1 Hz are presented in Fig. 3. In the green condition (Fig. 3A), wood type was a significant factor in explaining the differences in tan δ (F=5.49, p<0.001). A post hoc Tukey HSD test showed that species exhibiting a G-layer had a visibly and significantly higher tan δ in the TW than the OW. Differences between the mean tan δ of the TW and OW were 0.0091 for *Sextonia rubra* (p<0.001), 0.0105 for *O. guyanensis* (p<0.001) and 0.0080 for *I. alba* (p<0.001). In the air-dried condition (Fig. 3B), the general trend was for a decrease in tan δ, but wood type remained a significant factor (F=4.61, p<0.001) for the differences in tan δ, and there were significant differences between the TW and OW of two of the G-layer species: 0.0037 for *O. guyanensis* (p<0.001) and 0.0063 for *I. alba* (p<0.001). There were no significant differences in the air-dried tan δ of the non-G-layer species, and upon drying, there was no longer a significant difference in tan δ of the TW and OW of *S. rubra*. This trend can also be seen in the individual tree data (Table 2).

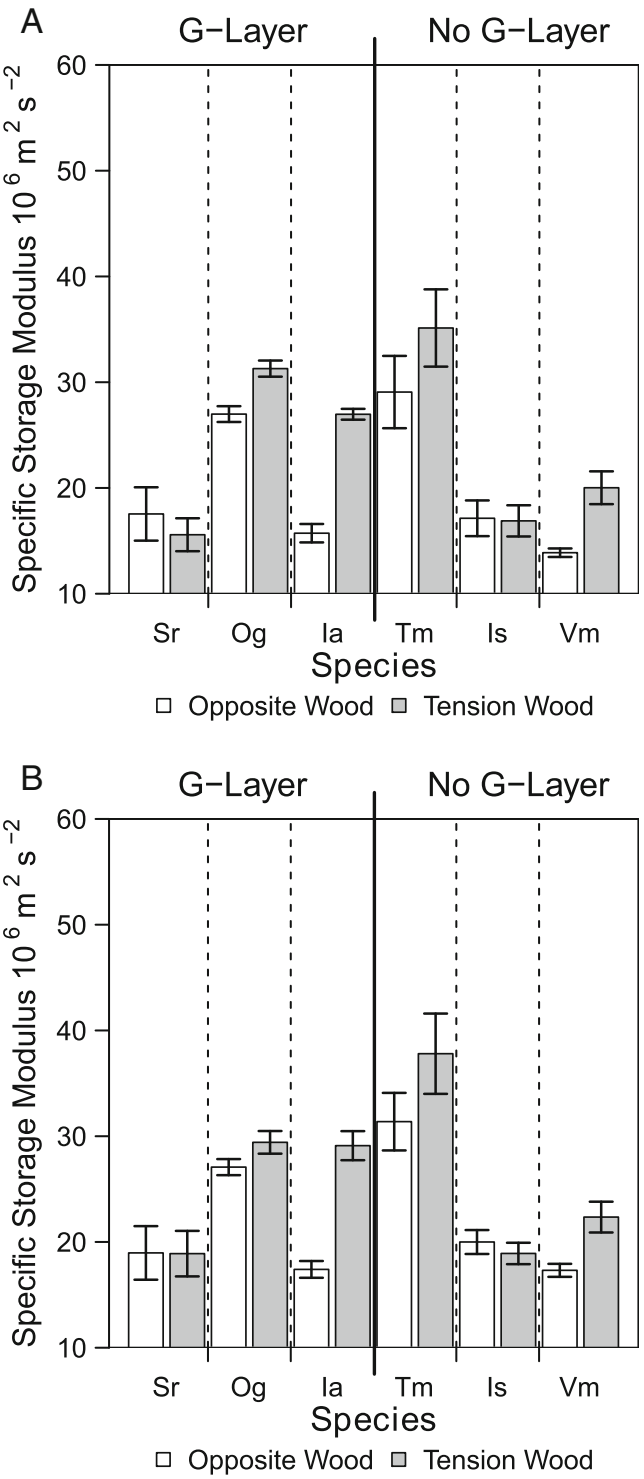

Fig. 2 Bar chart of mean specific tensile longitudinal storage modulus at 1 Hz by species and wood type for wood in the green condition (**A**) and dry condition (**B**). Error bars represent the standard error of the mean (n=6). Sr *Sextonia rubra*, Og *Ocotea guyanensis*, Is *Iyranthera sagotiana*, Vm *Virola michelii*, Ia *Inga alba*, Tm *Tachigali melinoni*

The mean values of longitudinal shrinkage between the green and oven-dried conditions are shown in Fig. 4. Wood type was a significant factor in explaining the differences in longitudinal shrinkage (F=12.45, p<0.001). A post hoc Tukey HSD test showed that those species that exhibited G-layer formation had visibly and significantly higher longitudinal shrinkage in the TW than the OW. Differences between the mean longitudinal shrinkage of the TW and OW were 0.45% (or TW shrunk 2.6 times more than OW) for *S. rubra* (p<0.001), 0.64% (or TW shrunk 4.0 times more than OW) for *O. guyanensis* (p<0.001) and 0.42% (or TW shrunk 2.9 times more than OW) for *I. alba* (p<0.001). No significant differences were found in the longitudinal shrinkage of the non-G-layer species.

Mean values of basic density are shown in Fig. 5. Wood type was a significant factor in explaining the differences in basic density (F=3.81, p<0.001). A post hoc Tukey HSD test showed that basic density of OW was higher than TW by 0.05 g cm^{-3} in *S. rubra* and 0.04 g cm^{-3} in *V. michelii*, whilst the TW had a higher basic density than the OW in *O. guyanensis* by 0.05 g cm^{-3}. Density values seemed to be fairly constant intra-species (Table 2), with the exception of *I. alba*.

Relationships between maturation stress, $E'\rho^{-1}$, tan δ and longitudinal shrinkage were examined, but no clear trends were observed, even when segregated by species and wood type (data not shown).

4 Discussion

The TW examined in this study did not always have a higher $E'\rho^{-1}$ (specific tensile storage modulus) than OW from the same tree. The observed $E'\rho^{-1}$ should be close to the specific tensile elastic modulus due to the observed cosine of δ being ~1; we can thus consider $E'\rho^{-1}$ as the specific stiffness of the measured samples. Furthermore, we can reasonably assume that tensile and flexural moduli of wood will show the same qualitative differences between wood types. Therefore, we can consider that a similar trend in wood specific modulus has been observed before in the literature. Ruelle et al. (2007) did not always find a significant difference between the air-dried specific flexural modulus of elasticity (MOE ρ^{-1}) of OW and TW in Guianese species. Of the ten species studied by Ruelle et al. (2007), only *O. guyanensis* was present in this study, and the same trend was observed (i.e. TW had a higher modulus than OW). The same authors presented a ratio of TW MOE ρ^{-1} over OW MOE ρ^{-1} for this species equal to 1.28; the same ratio applied here to $E'\rho^{-1}$ was 1.22 and thus comparable. The authors additionally presented ratios <1, which showed that the OW was stiffer than the TW for two species (*Virola surinamensis* and *Cecropia sciadophylla*). Furthermore, it is interesting that the maturation stresses showed no relationship to the specific tensile elastic storage modulus. MFA was not measured directly in this study, but considering the well-studied relationship between MFA and

Springer INRA

Table 2 Measured properties from each wood type and individual tree

Species	Tree	Wood type	Green tan δ	Air-dried tan δ	Green E'	Air-dried E'	ρ	LS	Green E'/ρ	Air-dried E'/ρ	Fibre type
Sextonia rubra	A	OW	**0.0170** (0.0008)	**0.0124** (0.0014)	***11,399*** (875)	**12,302** (369)	***0.53*** (0.01)	**0.23** (0.03)	**21,335** (1,746)	**23,006** (718)	G-layer
	A	TW	***0.0322*** (0.0046)	**0.0144** (0.0002)	**9,211** (965)	**11,619** (977)	**0.49** (0.02)	***0.90*** (0.20)	**18,555** (1,167)	**23,459** (1,035)	
	B	OW	**0.0200** (0.0008)	**0.0138** (0.0003)	**6,234** (357)	**6,910** (476)	***0.55*** (0.01)	**0.44** (0.06)	**11,409** (619)	**12,631** (733)	
	B	TW	**0.0217** (0.0018)	**0.0128** (0.0003)	**5,958** (796)	**6,763** (685)	**0.47** (0.02)	***0.60*** (0.08)	**12,598** (1,372)	**14,334** (1,119)	
Ocotea guyanensis	A	OW	**0.0143** (0.0001)	**0.0100** (0.0002)	**10,665** (476)	**11,322** (300)	**0.40** (0.00)	**0.21** (0.02)	**26,516** (1,149)	**28,155** (776)	
	A	TW	***0.0278*** (0.0010)	***0.0157*** (0.0002)	**11,741** (918)	**11,937** (1336)	**0.39** (0.02)	***0.92*** (0.04)	**30,070** (859)	**30,461** (1,912)	
	B	OW	**0.0134** (0.0003)	**0.0132** (0.0014)	**12,401** (604)	**11,758** (692)	**0.45** (0.02)	**0.21** (0.01)	**27454** (1,116)	**26,001** (1,065)	
	B	TW	***0.0189*** (0.0004)	**0.0154** (0.0007)	***18,085*** (898)	***15,789*** (835)	***0.56*** (0.01)	***0.80*** (0.09)	***32,502*** (830)	**28,381** (1,000)	
Inga alba	A	OW	**0.0175** (0.0004)	**0.0112** (0.0009)	**10,467** (111)	**11,049** (188)	**0.60** (0.03)	**0.22** (0.01)	**17,396** (728)	**18,402** (1,169)	
	A	TW	***0.0259*** (0.0020)	***0.0210*** (0.0040)	***18,710*** (621)	***20,905*** (1198)	***0.67*** (0.01)	***0.70*** (0.04)	***27,764*** (806)	***31,107*** (2,331)	
	B	OW	**0.0178** (0.0006)	**0.0099** (0.0003)	**6,766** (352)	**7,906** (489)	***0.48*** (0.01)	**0.23** (0.02)	**14,048** (681)	**16,408** (888)	
	B	TW	***0.0242*** (0.0006)	***0.0130*** (0.0011)	***10,348*** (296)	***10,714*** (248)	**0.40** (0.01)	***0.60*** (0.05)	***26,172*** (143)	***27,104*** (123)	
Tachigali melinoni	A	OW	**0.0205** (0.0013)	**0.0106** (0.0003)	**14,857** (268)	**14,967** (226)	**0.44** (0.05)	**0.39** (0.11)	**34,405** (4,070)	**34,737** (4,430)	No G-layer
	A	TW	**0.0194** (0.0009)	**0.0108** (0.0007)	**13,550** (318)	**14,698** (309)	**0.42** (0.02)	**0.29** (0.06)	**32,639** (2,475)	**35,399** (2,617)	
	B	OW	***0.0294*** (0.0047)	**0.0093** (0.0004)	**11,527** (2233)	**13,551** (1735)	***0.48*** (0.02)	**0.26** (0.07)	**23,732** (3,659)	**28,018** (2,474)	
	B	TW	**0.0210** (0.0023)	***0.0123*** (0.0017)	***15,438*** (2050)	***16,505*** (2105)	**0.42** (0.04)	**0.23** (0.02)	***37,613*** (7,379)	***40,204*** (7,712)	
Iriantera sagotiana	A	OW	**0.0178** (0.0009)	**0.0120** (0.0007)	**7,129** (291)	**9,610** (471)	**0.53** (0.00)	**0.48** (0.18)	**13,457** (599)	**18,142** (965)	
	A	TW	**0.0177** (0.0004)	**0.0127** (0.0013)	**7,587** (394)	**9,341** (482)	**0.55** (0.00)	**0.34** (0.04)	**13,738** (792)	**16,912** (938)	
	B	OW	**0.0140** (0.0008)	**0.0111** (0.0009)	**11,699** (113)	**12,746** (353)	**0.59** (0.00)	**0.08** (0.02)	**19,859** (148)	**21,636** (585)	
	B	TW	**0.0139** (0)	**0.0112** (0.0001)	**11,321** (455)	**11,814** (388)	**0.56** (0.01)	**0.11** (0.01)	**20,037** (583)	**20,916** (482)	
Virola michelli	A	OW	**0.0156** (0.0004)	**0.0137** (0.0010)	**7,178** (199)	**8,184** (429)	***0.49*** (0.01)	**0.24** (0.02)	**14,548** (483)	**16,597** (1,017)	
	A	TW	**0.0199** (0.0032)	**0.0141** (0.0011)	**7,155** (231)	**8,238** (94)	**0.43** (0.01)	**0.35** (0.05)	**16597** (269)	**19,130** (423)	
	B	OW	**0.0248** (0.0015)	**0.0159** (0.0008)	**6,512** (78)	**8,824** (387)	**0.46** (0.01)	***0.47*** (0.03)	**14,274** (362)	**19,320** (586)	
	B	TW	**0.0191** (0.0006)	**0.0144** (0.0010)	***10,127*** (310)	***11,059*** (434)	**0.43** (0.01)	**0.33** (0.02)	***23,442*** (493)	***25,575*** (185)	

Tan δ is the loss angle or longitudinal damping coefficient, E' is storage (elastic) longitudinal modulus (in gigapascals), ρ is basic density (in grams per cubic metre), LS is longitudinal shrinkage between the green and air dry condition (in per cent). Means (n=3) are given in bold and standard deviations in parentheses. Viscoelastic properties were measured using a sinusoidal tensile deformation at a frequency of 1 Hz and an ambient temperature of 30°C. Samples in the green condition were submerged. An underlined value signifies that it was significantly (α=0.05) higher than the corresponding wood type from the same tree (significance was determined by ANOVA)

TW tension wood, OW opposite wood

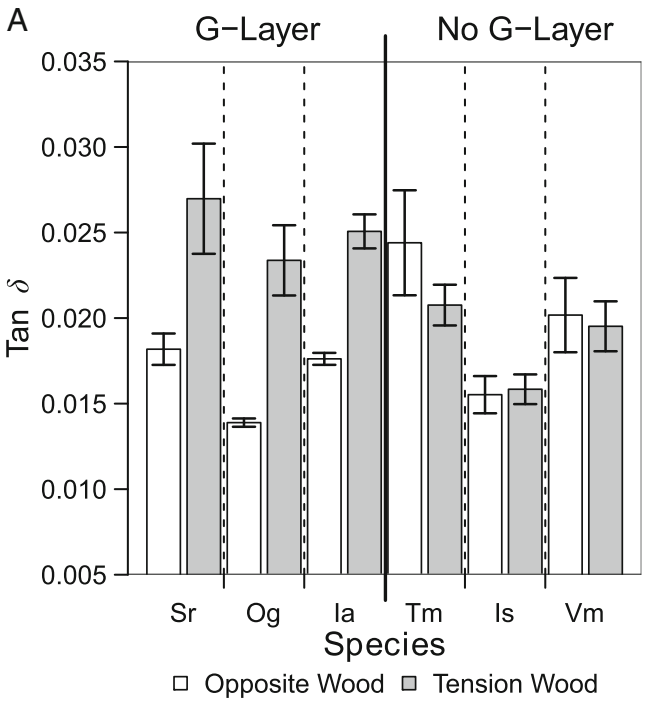

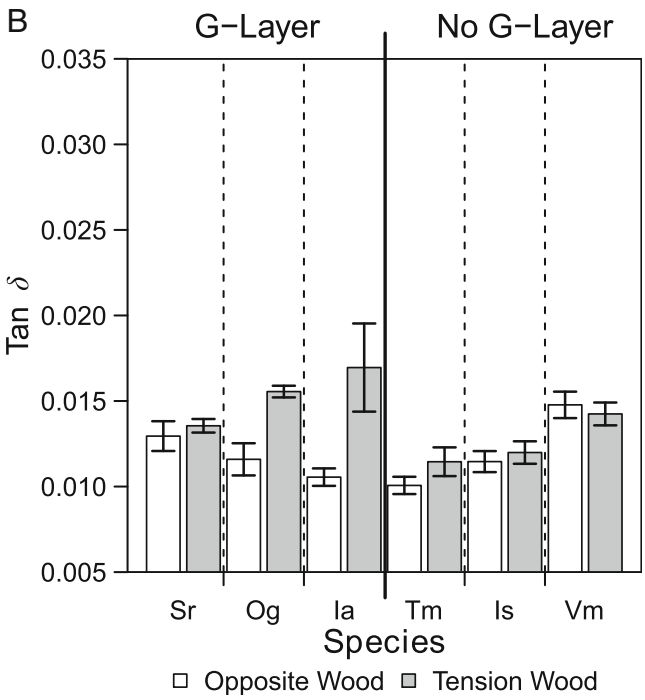

Fig. 3 Bar chart of mean tensile longitudinal tan δ at 1 Hz by species and wood type in the green (**A**) and air-dried condition (**B**). Error bars represent the standard error of the mean (n=6). Sr *Sextonia rubra*, Og *Ocotea guyanensis*, Is *Iyranthera sagotiana*, Vm *Virola michelii*, Ia *Inga alba*, Tm *Tachigali melinoni*

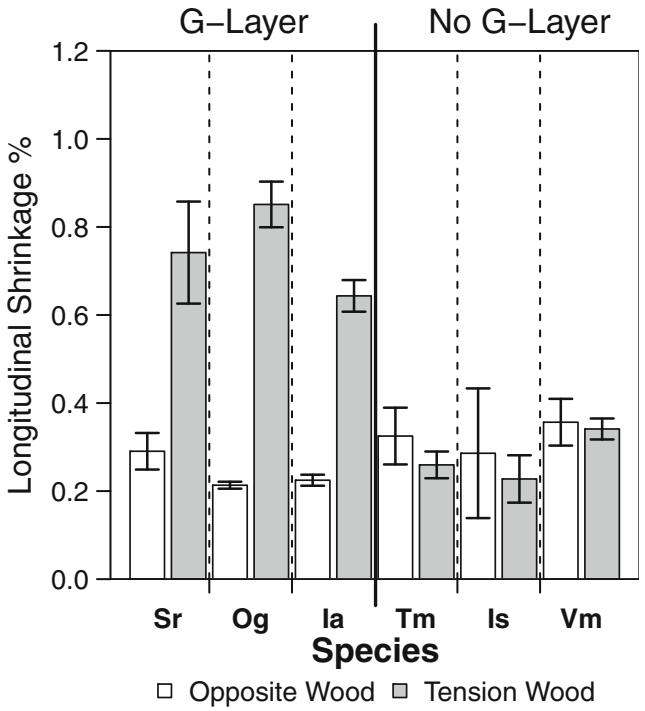

Fig. 4 Bar chart of mean longitudinal shrinkage by species and wood type between the green and oven dry condition. Error bars represent the standard error of the mean (n=6). Sr *Sextonia rubra*, Og *Ocotea guyanensis*, Is *Iyranthera sagotiana*, Vm *Virola michelii*, Ia *Inga alba*, Tm *Tachigali melinoni*

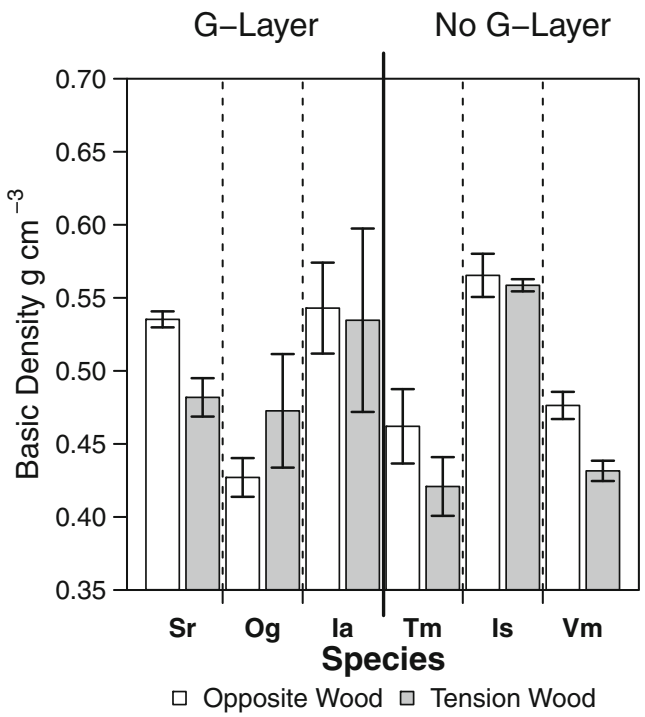

Fig. 5 Bar chart of mean basic density (oven dry mass/green volume) by species and wood type between the green and oven dry condition. Error bars represent the standard error of the mean (n=6). Sr *Sextonia rubra*, Og *Ocotea guyanensis*, Is *Iyranthera sagotiana*, Vm *Virola michelii*, Ia *Inga alba*, Tm *Tachigali melinoni*

elasticity (Cowdrey and Preston 1966), it can be deduced that there is quite possibly no simple relationship between the maturation stresses and MFA. This could be further evidence that MFA alone is not responsible for generating the tensile

forces associated with stem uprighting. This was previously proposed by Ruelle et al. (2007) who further suggested that "maturation strain is not strictly linked to MFA, but as much (or even more) to the chemical process of maturation".

The higher longitudinal shrinkage observed in the G-layer TW is similarly unrelated to the specific elastic modulus, which again can be taken as a proxy for MFA. The literature shows that having a low MFA is a characteristic of the G-layer (Daniel et al. 2006; Wada et al. 1995), as is high longitudinal shrinkage (Clair and Thibaut 2001). This does not follow the positive MFA and shrinkage relationship observed by Meylan (1972). Furthermore, Clair et al. (2008) have previously demonstrated that this high longitudinal shrinkage was due to the collapse of the mesoporosity of the G-layer. The fact that the non-G-layer TW did not have higher shrinkage than the OW in this study may not be true across all species, as Ruelle et al. (2007) previously observed a large (two times) difference in non-G-layer TW of *Simarouba amara*. However, in the same study, the shrinkage for *S. amara* TW was well below that of the G-layer TW of *Eperua falcata* or *O. guyanensis*, where the TW longitudinal shrinkage was greater than four times that of the corresponding OW. Whilst it is therefore not possible to state that there is definitely no difference in shrinkage between non-G-layer TW and OW, the fact remains that this result demonstrates that longitudinal shrinkage can be usefully employed as a method to differentiate between TW containing a G-layer and TW not containing a G-layer. The difference in shrinkage between the G-layer TW and OW is obviously, at least for the species examined, of a greater magnitude than any difference that may exist in longitudinal shrinkage between non-G-layer TW and OW.

For the species investigated, the TW of those with a G-layer was observed to have higher macroscopic damping relative to the OW of the same tree. This was not the case for species without a G-layer. Within the context of the current study, we cannot be sure whether or not this damping plays a direct biomechanical role for the tree or whether it is indicative of another biomechanical function. However, it is possible to speculate on the origin or origins of this damping within the material. For example, xyloglucan is thought to occur in the G-layer (Baba et al. 2009; Nishikubo et al. 2007), but not in typical lignified secondary cell walls. This polymer is thought to cross-link cellulose microfibrils in the primary cell wall (Bootten et al. 2004) and could cross-link the cellulose microfibrils on the surface of the G-layer with those on the adjacent S2 layer (Baba et al. 2009; Mellerowicz et al. 2008; Nishikubo et al. 2007). During tensile strain, a viscous (shear) deformation at the interface between the G-layer and the S2 layer, thus unique to fibres containing a G-layer, could occur and may explain the higher macroscopic damping of TW compared with OW within the same species. Furthermore, the absence of lignin in the G-layer may allow for the greater deformation of the polysaccharides between the cellulose molecules. Alternatively, if a shear lag effect (Young et al. 2004) is present in wood, as proposed by Montero et al. (2011), then axial loading of the G-layer, which is presumed to be stiffer than the normal secondary cell wall due to the abundance of cellulose (Daniel et al. 2006) and low MFA (Clair et al. 2011), could lead to a higher strain concentration at the interconnecting fibre ends. In this case, higher localised strains, relative to non-G-layer fibres, in the cellulose poor compound middle lamella (Roger et al. 2005) may result in viscous deformations and be manifested in higher macroscopic damping.

It is not clear why some species have developed the G-layer strategy in TW whilst others have not. On an evolutionary timescale, it appears that both sets of species appeared at similar times, but when a species has developed the G-layer, it has subsequently retained it (Ruelle J, 2009, presonal communication). Therefore, it may be a better (e.g. more efficient) system of stress generation. Clearly, there is more interesting research to be done on the diversity of tension wood and stem reorientation biomechanics. Future research should focus on matrix chemistry, micromechanics and the relationship between the wood matrix and maturation stress production.

5 Conclusion

The presence of a G-layer in the tension wood of the studied species was accompanied by an increased damping coefficient and notably higher longitudinal shrinkage relative to the respective opposite wood. Therefore, DMA and shrinkage measurements can provide a means of detecting G-layer material. The contribution of the G-layer matrix to damping and to maturation stress generation should be further studied.

Acknowledgements This project was supported by the French National Research Agency (ANR05 BDIV 012 04–WOODIVERSITY) and a joint project JSPS-CNRS. We thank Professor Yamamoto, K. Abe and J. Ruelle (Nagoya University, Japan) for help in field measurements and sample collection; Soepe Koese for sample preparation at the CIRAD facility in Kourou (French Guyana); and Professor Philip Harris (University of Auckland, New Zealand) for discussions about cell wall compositions. Finally, Gilles Camp from LMGC, University of Montpellier 2, is gratefully acknowledged for building the water bath and other necessary additions to the DMA apparatus.

References

Baba K, Park YW, Kaku T, Kaida R, Takeuchi M, Yoshida M, Hosoo Y, Ojio Y, Okuyama T, Taniguchi T, Ohmiya Y, Kondo T, Shani Z, Shoseyov O, Awano T, Serada S, Norioka N, Norioka S, Hayashi T (2009) Xyloglucan for generating tensile stress to bend tree stem. Mol Plant 2:893–903. doi:doi:10.1093/mp/ssp054

Bootten TJ, Harris PJ, Melton LD, Newman RH (2004) Solid-state ^{13}C-NMR spectroscopy shows that the xyloglucans in the primary cell walls of mung bean (*Vigna radiata* L.) occur in different domains: a new model for xyloglucan–cellulose interactions in the cell wall. J Exp Bot 55:571–583. doi:10.1093/jxb/erh065

Bruchert F, Speck O, Spatz HC (2003) Oscillations of plants' stems and their damping: theory and experimentation. Philos Transac Royal Soc Lond Ser B—Biol Sci 358:1487–1492. doi:10.1098/rstb.2003.1348

Cave ID (1968) Anisotropic elasticity of plant cell wall. Wood Sci Technol 2:268

Chang SS, Clair B, Ruelle J, Beauchene J, Di Renzo F, Quignard F, Zhao GJ, Yamamoto H, Gril J (2009) Mesoporosity as a new parameter for understanding tension stress generation in trees. J Exp Bot 60:3023–3030. doi:10.1093/jxb/erp133

Clair B, Thibaut B (2001) Shrinkage of the gelatinous layer of poplar and beech tension wood. IAWA J 22:121–131

Clair B, Ruelle J, Thibaut B (2003) Relationship between growth stress, mechanical–physical properties and proportion of fibre with gelatinous layer in chestnut (*Castanea sativa* Mill.). Holzforschung 57:189–195

Clair B, Ruelle J, Beauchene J, Prevost MF, Fournier M (2006) Tension wood and opposite wood in 21 tropical rain forest species 1. Occurrence and efficiency of the G-layer. IAWA J 27:329–338

Clair B, Gril J, Di Renzo F, Yamamoto H, Quignard F (2008) Characterization of a gel in the cell wall to elucidate the paradoxical shrinkage of tension wood. Biomacromolecules 9:494–498. doi:10.1021/bm700987q

Clair B, Almeras T, Pilate G, Jullien D, Sugiyama J, Riekel C (2011) Maturation stress generation in poplar tension wood studied by synchrotron radiation microdiffraction. Plant Physiol 155:562–570. doi:10.1104/pp.110.167270

Coutand C, Jeronimidis G, Chanson B, Loup C (2004) Comparison of mechanical properties of tension and opposite wood in *Populus*. Wood Sci Technol 38:11–24. doi:10.1007/s00226-003-0194-4

Cowdrey DR, Preston RD (1966) Elasticity and microfibrillar angle in the wood of Sitka spruce. Proc R Soc London, Ser B 166:245–272. doi:10.1098/rspb.1966.0097

Daniel G, Filonova L, Kallas AM, Teeri TT (2006) Morphological and chemical characterisation of the G-layer in tension wood fibres of *Populus tremula* and *Betula verrucosa*: labelling with cellulose-binding module CBM1(HjCel7A) and fluorescence and FE-SEM microscopy. Holzforschung 60:618–624. doi:10.1515/hf2006.104

R Development Core Team (2011) R: a language and environment for statistical computing. R Foundation for Statistical Computing, Vienna, Austria. ISBN 3-900051-07-0. http://www.R-project.org/

Donaldson LA (2001) Lignification and lignin topochemistry—an ultrastructural view. Phytochemistry 57:859–873

Fang CH, Clair B, Gril J, Liu SQ (2008) Growth stresses are highly controlled by the amount of G-layer in poplar tension wood. IAWA J 29:237–246

Fengel D, Wegener G (1984) Wood: chemistry, ultrastructure, reactions. Walter de Gruyter, Berlin

Fisher JB, Stevenson JW (1981) Occurrence of reaction wood in branches of dicotyledons and its role in tree architecture. Bot Gaz 142:82–95

Joseleau JP, Imai T, Kuroda K, Ruel K (2004) Detection in situ and characterization of lignin in the G-layer of tension wood fibres of *Populus* deltoides. Planta 219:338–345. doi:10.1007/s00425-004-1226-5

Jourez B, Riboux A, Leclercq A (2001) Anatomical characteristics of tension wood and opposite wood in young inclined stems of poplar (*Populus euramericana* cv 'Ghoy'). IAWA J 22:133–157

Jullien D, Gril J (2008) Growth strain assessment at the periphery of small-diameter trees using the two-grooves method: influence of operating parameters estimated by numerical simulations. Wood Sci Technol 42:551–565. doi:10.1007/s00226-008-0202-9

Mellerowicz EJ, Immerzeel P, Hayashi T (2008) Xyloglucan: the molecular muscle of trees. Ann Bot 102:659–665. doi:10.1093/aob/mcn170

Menard KP (2008) Dynamic mechanical analysis: a practical introduction. CRC, Boca Raton

Meylan BA (1972) The influence of microfibril angle on the longitudinal shrinkage–moisture content relationship. Wood Sci Technol 6:293–301. doi:10.1007/bf00357051

Montero C, Clair B, Alméras T, van der Lee A, Gril J (2011) Relationship between wood elastic strain under bending and cellulose crystal strain. Comp Sci Technol. doi:10.1016/j.compscitech.2011.10.014

Moore JR, Maguire DA (2008) Simulating the dynamic behavior of Douglas-fir trees under applied loads by the finite element method. Tree Physiol 28:75–83. doi:10.1093/treephys/28.1.75

Navi P, Stanzl-Tschegg S (2009) Micromechanics of creep and relaxation of wood. A review COST Action E35 2004–2008: Wood machining—micromechanics and fracture. Holzforschung 63:186–195. doi:10.1515/hf.2009.013

Nishikubo N, Awano T, Banasiak A, Bourquin V, Ibatullin F, Funada R, Brumer H, Teeri TT, Hayashi T, Sundberg B, Mellerowicz EJ (2007) Xyloglucan endo-transglycosylase (XET) functions in gelatinous layers of tension wood fibers in poplar—a glimpse into the mechanism of the balancing act of trees. Plant Cell Physiol 48:843–855. doi:10.1093/pcp/pcm055

Norberg PH, Meier H (1966) Physical and chemical properties of gelatinous layer in tension wood fibres of aspen (*Populus tremula* L.). Holzforschung 20:174–178

Onaka F (1949) Studies on compression and tension wood. Wood research bulletin. Kyoto University, Japan

Roger P, Mandla T, James H, Roger R, Jeffrey R (2005) Cell wall chemistry. In: Rowell RM (ed) Handbook of wood chemistry and wood composites. CRC, Boca Raton. doi:10.1201/9780203492437.ch3

Ruelle J, Clair B, Beauchene J, Prevost MF, Fournier M (2006) Tension wood and opposite wood in 21 tropical rain forest species 2. Comparison of some anatomical and ultrastructural criteria. IAWA J 27:341–376

Ruelle J, Beauchene J, Thibaut A, Thibaut B (2007) Comparison of physical and mechanical properties of tension and opposite wood from ten tropical rainforest trees from different species. Ann For Sci 64:503–510. doi:10.1051/forest:2007027

Salmen L, Burgert I (2009) Cell wall features with regard to mechanical performance. A review COST Action E35 2004–2008: Wood machining—micromechanics and fracture. Holzforschung 63:121–129. doi:10.1515/hf.2009.011

Sun N, Das S, Frazier CE (2007) Dynamic mechanical analysis of dry wood: linear viscoelastic response region and effects of minor moisture changes. Holzforschung 61:28–33. doi:10.1515/hf.2007.006

Tanaka F, Koshijima T, Okamura K (1981) Characterization of cellulose in compression and opposite woods of a *Pinus densiflora* tree grown under the influence of strong wind. Wood Sci Technol 15:265–273. doi:10.1007/bf00350944

Trenard Y, Gueneau P (1975) Relations between growth stresses and tension wood in beech. Holzforschung 29:217–223

Wada M, Okano T, Sugiyama J, Horii F (1995) Characterization of tension and normally lignified wood cellulose in *Populus maximowiczii*. Cellulose 2:223–233. doi:10.1007/bf00811814

Wardrop AB (1964) The reaction anatomy of arborescent angiosperms. In: Zimmerman MH (ed) The formation of wood in forest tree. Academic, New York, pp 405–456

Yoshida M, Okuyama T (2002) Techniques for measuring growth stress on the xylem surface using strain and dial gauges. Holzforschung 56:461–467

Yoshida M, Okuda T, Okuyama T (2000) Tension wood and growth stress induced by artificial inclination in *Liriodendron tulipifera* Linn. and *Prunus spachiana* Kitamura f. *ascendens* Kitamura. Ann For Sci 57:739–746

Young RJ, Eichhorn SJ, Shyng YT, Riekel C, Davies RJ (2004) Analysis of stress transfer in two-phase polymer systems using synchrotron microfocus X-ray diffraction. Macromolecules 37:9503–9509. doi:10.1021/ma048484x